Dalton Transactions

ROYAL SOCIETY OF CHEMISTRY

PAPER

View Article Online
View Journal | View Issue

Cite this: *Dalton Trans.*, 2024, **53**, 13795

Phenalenyl-ruthenium synergism for effectual catalytic transformations of primary amines to amides†

Nilaj Bandopadhyay,[a] Krishnendu Paramanik,[a] Gayetri Sarkar,[a] Suvojit Roy,[a] Subhra Jyoti Panda,[b] Chandra Shekhar Purohit,[b] Bhaskar Biswas *[a] and Hari Sankar Das *[a]

The synthesis of amides holds great promise owing to their impeccable contributions as building blocks for highly valued functional derivatives. Herein, we disclose the design, synthesis and crystal structure of a mixed-ligand ruthenium(II) complex, [Ru(η^6-Cym)(O,O-PLY)Cl], (**1**) where Cym = 1-isopropyl-4-methyl-benzene and O,O-PLY = deprotonated form of 9-hydroxy phenalenone (HO,O-PLY). The complex catalyzes the aerobic oxidation of various primary amines (RCH_2NH_2) to value-added amides ($RCONH_2$) with excellent selectivity and efficiency under relatively mild conditions with common organic functional group tolerance. Structural, electrochemical, spectroscopic, and computational studies substantiate that the synergism between the redox-active ruthenium and π-Lewis acidic PLY moieties facilitate the catalytic oxidation of amines to amides. Additionally, the isolation and characterization of key intermediates during catalysis confirm two successive dehydrogenation steps leading to nitrile, which subsequently transform to the desired amide through hydration. The present synthetic approach is also extended to substitution-dependent tuning at PLY to tune the electronic nature of **1** and to assess substituent-mediated catalytic performance. The effect of substitution at the PLY moiety (5th position) leads to structural isomers, which were further evaluated for the catalytic transformations of amine to amides under similar reaction conditions.

Received 17th June 2024,
Accepted 15th July 2024

DOI: 10.1039/d4dt01760a

rsc.li/dalton

Introduction

The synthesis of amides remains one of the most imperative transformations for delivering value-added chemicals in the chemical and pharmaceutical industries.[1–6] The amide is a key functional group in organic chemistry and abundant in the biological world.[7–9] Notably, amides are extensively used as intermediates in synthetic organic chemistry.[1,2] It is evident that ≈25% of the available drugs are based on amide functionality.[10] Typically, the ideal amide synthetic method involving the condensation of carboxylic acid and amine generates only one equivalent water as a byproduct. This synthetic approach is not feasible under ambient conditions owing to the proton transfer from the acid to amine, leading to an ammonium carboxylate salt.[11] An external stimulator such as heat or light[12–14] is required to achieve this coupling reaction, which makes the process incompatible with the chemical complexity exhibited by modern drug molecules. Amides are traditionally synthesized by condensing carboxylic acid derivatives with electronically deficient carbonyl carbon, such as acid chlorides, anhydrides, and esters with amines or *via* acid-catalyzed Beckmann rearrangement of ketoximes under relatively mild conditions to avoid proton transfer issues.[15,16] However, these traditional methods suffer from the use of stoichiometric quantities of various hazardous reagents, leading to equimolar amounts of by-products. Therefore, developing an atom-economic and sustainable synthetic approach towards amide synthesis is highly desirable in modern synthetic organic chemistry. Consequently, several methods for amide synthesis have been designed and developed in the last few decades, including the dehydrogenative amidation of alcohol,[10,17–27] aminocarbonylation of aryl halides,[28–32] hydroamination of alkynes,[33–36] transamidation of primary carboxamides,[37–43] oxidative amidation of aldehydes,[44–53] catalytic rearrangement of oximes,[54–59] and hydration of nitriles.[60–66] In this context, the selective α-oxygenation of primary amines using molecular O_2 (from the air) as the terminal oxidant where H_2O is the only by-product has been considered one of the most promising and sustainable routes to yield amides[67,68] as amines are readily available through a wide number of common organic

[a]*Department of Chemistry, University of North Bengal, Darjeeling 734013, India. E-mail: harisankardas@nbu.ac.in, bhaskarbiswas@nbu.ac.in*
[b]*Department of Chemical Sciences, National Institute of Science Education and Research, Bhubaneswar, Orissa-751005, India*

†Electronic supplementary information (ESI) available. CCDC 2246583, 2331544 and 2332941 for complex **1**, **2**, and **3**. For ESI and crystallographic data in CIF or other electronic format see DOI: https://doi.org/10.1039/d4dt01760a

transformations.[69–76] However, this selective α-oxygenation of primary amine is highly challenging owing to the moderate reactivity of C–H bonds of α-carbon compared to the higher reactivity of the $-NH_2$ group. In contrast, molecular O_2 in its triplet ground state is thermodynamically stable and needs activation before the reaction.[77] In the context of α-oxygenation of primary amines using aerial O_2, the first efforts were made by Mizuno in 2008 using a heterogeneous catalyst $Ru(OH)_x/Al_2O_3$.[78] Thereafter, several efficient heterogeneous metal-based catalysts have been reported in the literature (Scheme 1), such as Au-nanoparticles,[79–81] Au-nanoclusters,[82] PVP-stabilized nanogold,[83] MnO_2-based octahedral molecular sieves (OMS-2),[84] manganese oxide nanorods ($NR\text{-}MnO_x$),[85] and Au/Al_2O_3,[86] for the aerial oxidation of amines to amides. However, in these methods, including the first report, the amine-to-amide transformation sufferers either from the use of a high-pressure reactor under pressurized air-oxygen (≥5 atm) at an elevated temperature (130–160 °C) and/or from the limited substrate scope with low selectivity. On the contrary, researchers have devoted significant efforts to homogeneous catalysis to increase selectivity and to elevate the efficiency of the reaction (Scheme 1). In 2012, Fu and co-workers first introduced a homogeneous copper(I) catalyst for aerobic oxidation of (aryl)methanamines to the corresponding primary amides using aerial O_2 as oxidant in DMSO–H_2O containing 2 equivalents of K_2CO_3 base.[87] After that, in 2018, Lahiri and co-workers reported a commercially available homogeneous catalyst RuHCl(CO)$(PPh_3)_3$ for selective oxidation of benzylamine to amides under mild conditions with 1–2 equivalent of base loading in ^{t}BuOH.[88] Recently, Lin and co-workers demonstrated homogeneous selective oxygenation of primary amines to amides using an N,O-bidentate ligand-supported trinuclear ruthenium carbonyl cluster system under the presence of 1 equivalent base in refluxing ^{t}BuOH.[89] Further, Bera and co-workers have reported very recently a ruthenium-based efficient catalyst for aerobic oxidation of primary amines to amides under a mild condition in the presence of 30 mol% base loading.[90] Therefore, the development of novel and efficient catalytic systems for the aerobic oxidation of amines to amides and their way of action remains a deep concern.

In contrast, redox-active phenalenyl (PLY) moiety plays a pivotal role in the catalytic transformations of various organic functional groups.[91] Very recently, Mandal and co-workers successfully demonstrated the PLY-mediated hydrogen by borrowing from alcohol to aldehyde, followed by further transfer of borrowed hydrogen to imine to amine transformation.[92] As amine-to-amide transformation generally proceeds *via* a two-step mechanism, (i) dehydrogenation of amine to nitrile and (ii) hydration of nitrile to amide,[78,84,85,89,90] the PLY moiety may help in this challenging transformation of amine to nitrile by borrowing hydrogen from amine. It is also observed that the aerobic oxidation of primary amines to amides is carried out by ruthenium-based catalytic systems in most cases.[78,88–90] By maintaining all these pieces of information and as our general interest to develop catalytic organic trans-

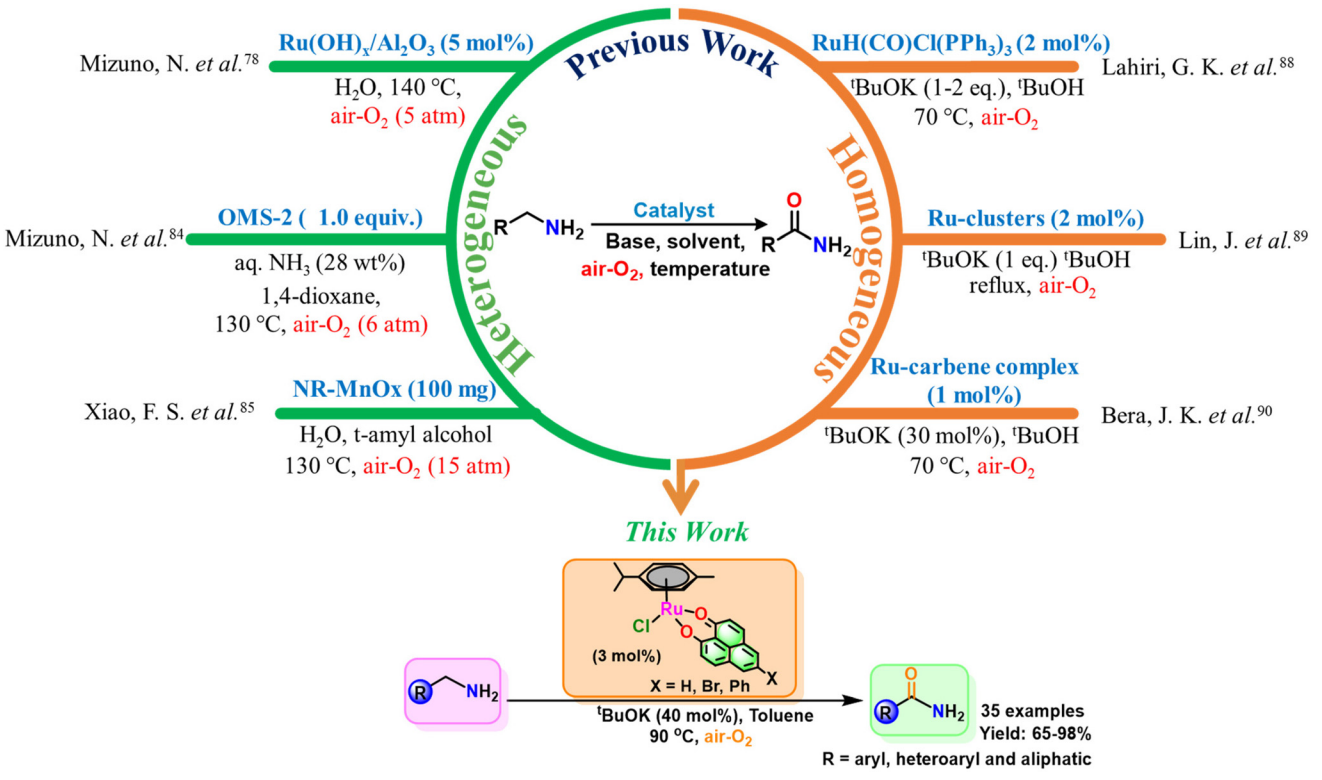

Scheme 1 Comparison of the present catalytic system with previous reports for the aerobic oxidation of amines to amide.

formations using coordinatively unsaturated metal complexes,[93–95] herein we report the synthesis, structural and electrochemical properties of different PLY-based ruthenium complexes of the form [Ru(η^6-Cym)(O,O-PLY)Cl], **1**, [Ru(η^6-Cym)(O,O-PLY-Br)Cl], **2**, and [Ru(η^6-Cym)(O,O-PLY-Ph)Cl], **3** and their potential application as a catalyst in aerobic oxidation of amine to amides. The newly designed complexes exhibit excellent catalytic activity towards aerobic oxidation of amine to amides under mild conditions (Scheme 1).

Results and discussion

Synthesis and structures of 1–3

The ruthenium(II)-cymene complex **1–3** was formed by stirring a 2 : 1 mixture of PLY-based ligands (HO,O-PLY, HO,O-PLY-Br and HO,O-PLY-Ph) and dimeric ruthenium precursor [Cl(η^6-Cym)Ru(μ-Cl)$_2$Ru(η^6-Cym)Cl] in DCM at room temperature (RT) in the presence of excess base NEt_3 (Fig. 1a). Complex **1–3** was isolated as reddish crystalline solids with excellent yields by slow evaporation of the reaction mixtures at RT. **1–3** is expectedly diamagnetic, air-stable and well soluble in common organic solvents. The analytical purity of **1–3** was determined by elemental analysis, NMR, IR, UV-Vis spectroscopy and mass spectrometry (Fig. S7–S17, ESI†). Single crystals of **1–3** suitable for X-ray diffraction studies were obtained by the slow evaporation of MeOH/DCM (3 : 1) solution at RT. Compounds **1** and **3** crystallized in the monoclinic lattice system with the $P2_1/n$ space group and **2** crystallized in the orthorhombic lattice system with the $P2_12_12_1$ space group (Table S1†).

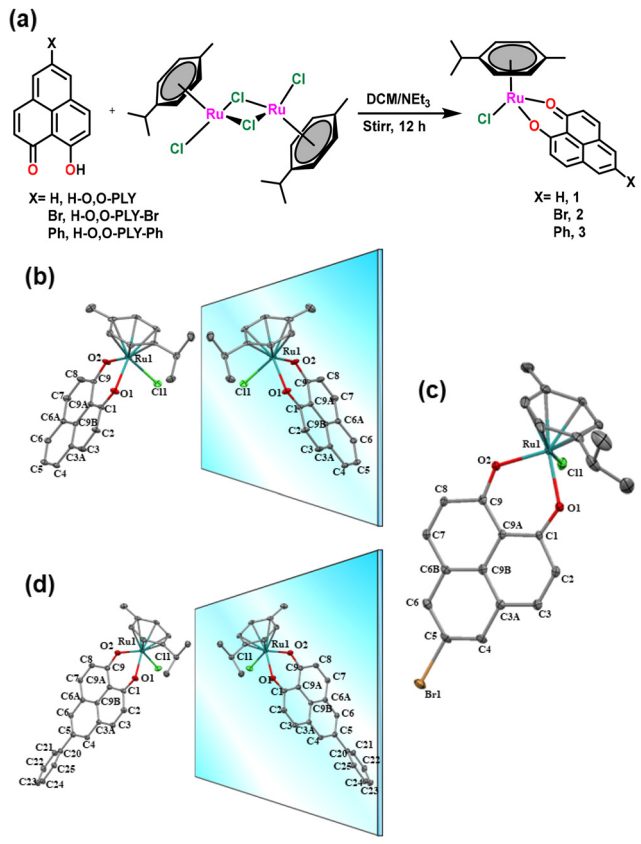

Fig. 1 (a) Synthetic scheme of complex **1–3**. (b–d) Perspective view of complex **1–3** with 50% thermal ellipsoidal probability. All the hydrogen atoms are omitted for clarity.

The ORTEP diagrams of neutral complex **1–3** are shown in Fig. 1b–d with an asymmetric unit containing a η^6-Cym, an O, O-donor PLY and a chloride ligand in a piano-stool structural fashion. The bond parameters associated with **1–3** are listed in Tables S2 and S3.† The Ru–O and Ru–Cl distances in **1–3** are in the expected range of such types of reported piano-stool complexes (Table S2†).[96] Small changes in Ru–O and C–O distances are observed when the 5th position of the PLY moiety is substituted, indicating some changes in its electronic nature. The Ru–C distances for all six arene carbon atoms in **1–3** are almost equivalent, with an average of 2.177(4) Å, confirming the η^6 coordination mode of the Cym ligand. The torsion angles of 38.12° (C6–C5–C20–C21) and 36.01° (C4–C5–C20–C25) in **3** between –Ph and PLY moieties are relatively lower than the reported torsion angles in an ideal biphenyl system (44.4°).[97] This accounts for better coplanarity and higher conjugation between –Ph and PLY moieties. In this type of cymene complex, two isomeric structures are possible depending on the orientation of the chloro ligand to the cymene-σ_v plane left or right. Both compounds **1** and **3** are present in two isomeric forms in the crystal structure that are mirror images of each other (Fig. 1b and d), while only one isomer was observed in the crystal structure of **2** (Fig. 1c). The presence of only one optical isomer indicates that compound **2** must be optically active. Circular dichroism (CD) analysis of compound **1–3** (Fig. S18–S20†) confirms the optical activity of **2**. To the best of our knowledge, this is the first report in which not only the electronic nature of the ruthenium-cymene system is changed but also the deracemization of the system occurs when a suitable bulky substituent is attached to an achiral symmetrical bidentate PLY ligand system.

Electrochemistry

The presence of two redox-active moieties (PLY and Ru) in **1–3** prompted us to investigate their redox properties by cyclic voltammetry (CV). Complex **1** shows one quasi-reversible oxidation at 1.27 V and two irreversible reductions at −1.26 V and −1.39 V (Fig. 2a and Table 1, *versus* Ag/AgCl) in DCM/0.1 M Bu_4NPF_6, (Fig. 2). On substitution of PLY 5th C–*H* by electron-withdrawing –Br or –Ph, the two reduction potentials of the complexes (**2** and **3**) shifted significantly, indicating that the two reduction steps are based on the PLY moiety (Fig. S21†). Interestingly, although the –Ph group has an electron-withdrawing nature, the –Ph-substituted PLY-complex **3** is reduced at potentials relatively higher than **1** (Fig. S21†). This could be due to the conjugation of the –Ph π-orbitals with the π-orbitals of the PLY moiety present in an almost coplanar situation (Fig. 1d), which makes the PLY moiety electronically rich. To verify this hypothesis, we also compared the reduction potential of ligand HO,O-PLY-Ph with HO,O-PLY and obtained the

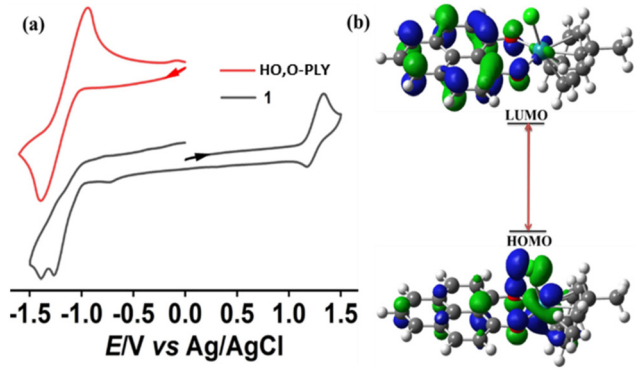

Fig. 2 (a) Cyclic voltammograms of **1** and HO,O-PLY in DCM/0.1 M Bu_4NPF_6 at 298 K *vs.* Ag/AgCl. (b) HOMO and LUMO of complex **1**.

Table 1 Redox potentials of complexes **1**, **2**, and **3** [a]

Complex	PLY-centered reduction		Ru-centered oxidation
	E^{red1}	E^{red2}	$E^{ox}_{1/2}$ (ΔE_P)
1	−1.26	−1.39	+1.27 (110)
2	−1.15	−1.27	+1.22 (70)
3	−1.49	−1.69	+1.19 (320)

[a] Electrochemical potential in V *vs.* Ag/AgCl from cyclic voltammetry in DCM/0.1 M Bu_4NPF_6 at 298 K. Scan rate: 100 mV s^{-1}

same result (Fig. S22†) observed in their metal complexes (Fig. S21†). The shift of the oxidation potential is comparatively less significant on substitution at PLY-moiety (Fig. S21†), so this process at +1.27 V is likely to be ruthenium cantered. Further, to assign the redox processes of **1**, a preliminary DFT calculation using the B3LYP method was performed (Fig. 2b). Oxidation involves the removal of an electron from the HOMO of the system, while reduction involves the addition of an electron to the LUMO of the system. The calculated frontier orbital HOMO and LUMO of **1** are located mainly on the ruthenium and PLY moiety, respectively, clearly suggesting that oxidation is ruthenium centred and the first reduction is PLY centred.

Catalytic studies

Inspired by the efficient catalytic activity of ruthenium complexes for the useful synthesis of amides from amine *via* α-oxygenation, first, we checked the catalytic activity of **1** (3 mol%) for α-oxygenation of primary amines to primary amides using air-O_2 as an oxidizing agent. **1**-Catalyzed aerial oxidation of model substrate benzylamine for 15 hours at 90 °C in toluene (Table S4,† entry 1) resulted in a very low yield of amide with several side products. Delightfully, on adding a catalytic amount of KO^{t}Bu (40 mol%), complex **1** (3 mol%) catalyzes the benzylamine to benzamide, **5a** selectively with 93% yield (Table S4,† entry 2). Notably, the formation of the desired amide was not detected (Table S4,† entry 3) in the absence of **1**, confirming the essential presence of **1** during catalysis. To validate the role of complex **1**, the catalytic transformation of amine to amide was carried out using a 1.5 mol% precursor complex $[Cl(\eta^6\text{-Cym})Ru(\mu\text{-Cl})_2Ru(\eta^6\text{-Cym})Cl]$. However, it yielded the desired amide only in less than 30% yield (Table S4,† entry 4). Additionally, the catalytic activity of the ligand HO,O-PLY (3 mol%) was tested, and only a trace amount of the desired product was formed (Table S4,† entry 5). Furthermore, the variation in the reaction parameters, such as catalyst loading, base loading, temperature, time and solvents (Table S4,† entries 6–18), resulted in no further improvement under the reaction conditions. The progress of the reactions was monitored by involving the amount of amide formed *versus* different time intervals (2, 4, 6, 8, 10, 12, 14, and 16 h), suggesting that the reaction progressed to completion within 14 hours (Fig. S23 and Table S5†). Subsequently, the optimized reaction conditions (toluene, 90 °C, 15 h, 3 mol% pre-catalyst **1**, and 40 mol% KO^{t}Bu) were implemented on a wide variety of substrates, including aryl-, biaryl-, heteroaryl- and aliphatic-methanamines, to assess the scope and generality of the present protocol (Table 2).

As shown in Table 2, benzylamines bearing electron-withdrawing groups (*e.g.*, –Br, –Cl, –F, $–CF_3$, $–OCF_3$, and $–NO_2$) were α-oxygenated to their corresponding primary amides (entry **5b–m**) efficiently in high to excellent yields (93–98%), while benzylamines substituted with electron-donating groups (*e.g.*, –Me, $–NH_2$, –OMe, –OEt and –OH,) proceeded with relatively low yields (65–71%, entry **5n–w**). Under the same reaction conditions, several biaryl-, heteroaryl- and bioactive heteroaryl-methanamines[90] were also α-oxygenated smoothly to their corresponding amides in good yields (82–94%, entry **6a–f**). To our delight, in the presence of excess base (KO^{t}Bu), the more challenging aliphatic primary amine substrates can also be oxygenated to primary amides using the same catalyst with moderate yields (64–92%, entry **6g–l**). Our α-oxygenation results demonstrate that in the present methodology, the common functional groups, including –Br, –Cl, –F, $–CF_3$, $–OCF_3$, $–NO_2$, –OH, $–NH_2$, –OMe, and –OEt, are tolerated (Table 2). Additionally, the amide synthesis from amine was scaled up to the gram scale, which resulted in an 85% yield for **5a** (Scheme S1†), highlighting the practical applicability of the current protocol. Next, to observe the effect of substitution dependence tuning at the PLY moiety of **1** in the present amine-to-amide transformation reaction, we implemented complexes **2** and **3** as catalysts in the oxidation of model substrate **4a** and obtained 87% and 98% yields of **5a**, respectively. This indicates that a system with an electronically rich PLY moiety (reduced at a higher potential) shows better catalytic activity than a system with an electronically deficient PLY moiety.

Mechanistic studies

After the successful application of the catalytic transformations to a broad substrate scope, we are keen to unveil the mechanistic pathways for catalysis. Previously, it was demonstrated that amine-to-amide transformation generally proceeds *via* two successive dehydrogenation steps (amine to imine and nitrile, respectively), followed by hydrating the key nitrile, leading to the desired amide.[79,84,88–90] In our method, when the base (KO^{t}Bu)-free amine to amide transformation was

Table 2 1-Catalysed aerobic oxidation of primary amines to primary amides[a,b]

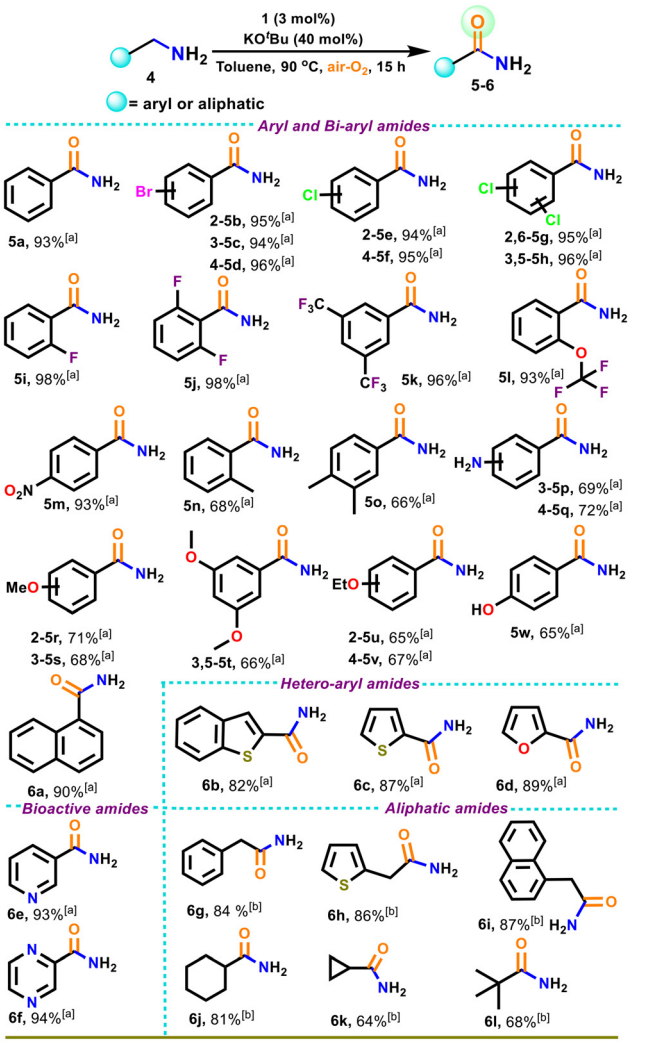

[a] Reaction conditions: amine (0.5 mmol), KO^{t}Bu (40 mol%), catalyst **1** (3 mol%), and toluene (3 mL) for 15 h at 90 °C under aerobic conditions, with isolated yields. [b] KO^{t}Bu (250 mol%) was used instead of 40 mol% under condition [a].

Scheme 2 1-Catalysed aerial oxidation of benzylamine (**4a**) in the absence of a base.

carried out in the presence of 2 mol% catalyst loading instead of 3 mol% to make the reaction slow, a mixture of products was formed. Analysis of the NMR spectra (Fig. S24–S29†) of the products after chromatographic separation confirms the presence of the desired amide, **5a**, along with imine (*N*-substituted), **7a**, and nitrile, **8a** (Scheme 2), demonstrating that the present reaction also proceeds through the same reaction path, as previously demonstrated.[79,84,88–90]

To confirm the nitrile as the key intermediate, we carried out further the transformation of nitrile to amide under our optimized condition, enabling the formation of the expected benzamide (**5a**) in 97% yield (Scheme S3†). However, it is reported that the base, KO^{t}Bu, can convert nitrile to primary amide stoichiometrically in the presence of an external proton source ^{t}BuOH.[59] Notably, in the present study, 40 mol% KO^{t}Bu is sufficient for the full conversion of **1** catalyzed nitrile to amide (Table S4,† entry 2). In the absence of catalyst **1**, the 40 mol% KO^{t}Bu affords only around 34% amide in the nitrile-to-amide transformation (Scheme S4†). In the absence of KO^{t}Bu, a partial transformation of amine to amide was observed in Scheme 2, indicating that catalyst **1** can hydrate nitrile. Such **1**-catalysed hydration was further verified through a labeling experiment using D_2O. The appearance of a mass peak at *m*/*z* 123 (Fig. S30†) ensures the complete insertion of D_2O into the nitrile intermediate. This information entrusts the crucial role of catalyst **1** in the nitrile-to-amide transformation. Besides, we performed the **1**-catalysed aerial oxidation of benzylamine in the presence of a radical scavenger, 2,2,6,6-tetramethylpiperidine-1-oxyl (TEMPO, excess). The excess TEMPO could not shut down the reaction completely (86% benzamide was isolated), implying a non-radical reaction pathway (Scheme S6†). UV/Vis spectroscopic measurements were performed to determine the interaction of catalyst **1** with all the reagents, such as amine, O_2 and KO^{t}Bu. No change in charge transfer bands at 515, 438, 414 and 350 nm was observed at room temperature, even when the mixtures were kept for a few hours (Fig. S31†). However, a clear change from reddish to greenish color was observed when **1** was treated with benzylamine at 90 °C under O_2-free conditions. The green solution shows a significant change in the PLY-centered charge transfer bands along with a new band appearing at around 665 nm (Fig. S32†), signifying the direct interaction of the amine with **1**. The ESI-MS spectrum of this green solution exhibits characteristic peaks at *m*/*z* 431 and 538, corresponding to the species $[Ru(\eta^6\text{-Cym})(O,O\text{-PLY})]^+$, **1a** and $[Ru(\eta^6\text{-Cym})(O,O\text{-PLY})(Ph\text{–}CH_2\text{–}NH_2)]^+$, **1b** respectively (Fig. S33†). To get more information about the key intermediates, we measured the reaction mixture's mass spectra during the progress of the reaction (Fig. S34†). On analysis of mass spectra, we found peaks at 431 and 538 for **1a** and **1b**, respectively, along with some additional peaks appearing at 579, 577 and 465. Both peaks appearing at 579 and 577 may be attributed to the generation of species $[Ru(\eta^6\text{-Cym})(O,O\text{-PLY-}H_2)(Ph\text{–}CH{=}NH)]^+$, **1d** (Fig. S34a and b†), and the peak appearing at 465 indicates the formation of species $[Ru(\eta^6\text{-Cym})(O,O\text{-PLY-}H_2)(O_2)]^+$, **1e** during the reaction (Fig. S34†). An intense mass peak at *m*/*z* 619 also appeared even after 6 hours of the reaction, which could be attributed to the presence of the catalyst-amine adduct, **1b** (Fig. S34†), suggesting the stability of the active unit during the reaction. The possibility of the formation of the $Ru^{IV}{=}O$ complex[88,90] during catalysis was also examined; however, it was excluded by observing that the mixture did not show any EPR signal at 100 K (Fig. S35†). It is noteworthy that Mandal

and co-workers recently demonstrated that the PLY moiety can borrow hydrogen from benzylic and aliphatic alcohols and store it on the PLY backbone, causing the oxidation of alcohol to aldehyde.[92] As benzylic amine is isoelectronic with benzylic alcohol, the present catalytic reaction may follow the same hydrogen borrowing mechanism. However, the hydrogen borrowing capability of the PLY moiety was observed only when PLY was present in the reduced state.[92] The present system is similar to the ruthenium-quinone system, where intense metal-to-ligand (quinone) charge transfer transitions (MLCT) are observed *via* d_π–p_π mixing.[98] In the present case, when complex **1** is treated with amine, an intense MLCT band at around 665 nm is evident (Fig. S32†). Such MLCT may lead to the formation of active species $[Ru^{III}(\eta^6\text{-Cym})(O,O\text{-PLY})^{\bullet-}(Ph–CH_2–NH_2)]^+$, **1c** where an electron from Ru^{II} is transferred to the PLY moiety, resulting in an active reduced PLY unit. To confirm the role of this 665 nm transition band in amine-to-amide transformation, we performed the reaction using a red-light source when a green reaction mixture obtained by heating at 90 °C for 15 minutes was used (Scheme S7†). In this method, the amide was isolated with a 74% yield. Next, we performed the reaction in the presence of sunlight instead of a red light source, resulting in an 81% yield of the desired amide (Scheme S8†). The same experiment was carried out under dark conditions and produced the desired amide with 32% yield (Scheme S9†), further validating the role of the 665 nm MLCT-band in the present catalytic transformation. Furthermore, we used the fluorescence spectroscopic technique to observe the effect of MLCT on ligand (PLY)-based emission. The free HO,O-PLY moiety shows intense emission when irradiated with visible light (Fig. S36a†). However, this emission becomes quenched when the PLY moiety is attached to Ru(II) in the complex, indicating electron transfer from Ru(II) to the PLY moiety (Fig. S36b†) during visible light irradiation. Based on all these experimental observations and analytical outcomes, a plausible reaction mechanism is proposed involving a non-radical pathway (Scheme 3).

First, the base KO^{t}Bu accelerates the dissociation of the ruthenium chloride bond of **1** and forms coordinatively unsaturated species **1a** (detected by ESI-MS, Fig. S33†).[99] After that, **1a** binds with amine, forming species **1b** (detected by ESI-MS, Fig. S33†). On heating or irradiation with light, an electron is transferred from Ru^{II} to redox-active PLY moiety, forming active species **1c**. Then, the reduced PLY moiety of **1c** borrows the hydrogen from the methanamine moiety to its backbone, followed by electron rearrangement, leading to the oxidation of amine to imine and the reduction of α,β-unsaturated C=C of the PLY backbone to two C–H bonds, as shown in **1d**. Next, aerial oxygen binds with **1d** and forms **1e**, which is detected by the appearance of a peak at *m*/*z* 465 in mass spectroscopy (Fig. S34†). Then, coordinated oxygen oxidised the reduced PLY-moiety to the native PLY moiety and was reduced to H_2O_2. The formation of H_2O_2 was detected indirectly by the iodide oxidation reaction described in the literature,[100–102] resulting in I^- to I_3^- being confirmed by the appearance of characteristic intense peaks at 285 and 353 nm (Fig. S36†).[103] Similarly,

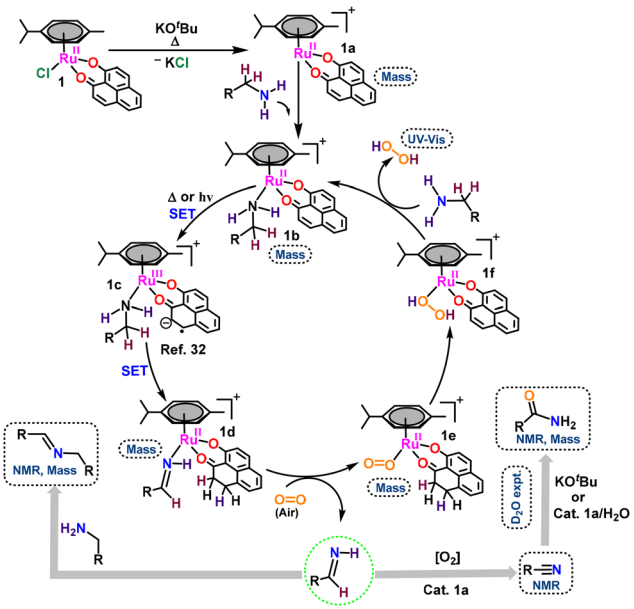

Scheme 3 Proposed Ru^{II}-PLY catalyzed α-oxygenation of amine to amide using aerial oxygen.

the imine is oxidized further to nitrile through the same reaction path, as depicted in amine-to-imine oxidation. Once nitrile is formed, the base KO^{t}Bu[59] or the catalyst **1a** (Scheme 3) converts it into amide.

Conclusion

In summary, we developed labile Ru-based catalysts (**1–3**) in the form $[Ru(\eta^6\text{-Cym})(PLY)Cl]$ by combining a ruthenium-cymene precursor and different substituted redox-active phenalenyl (PLY)-based ligands to monitor the synergistic effect in the catalytic transformations of amine to amide. Structural analysis of these complexes demonstrates the η^6-coordination mode of the cymene ligand and mono-deprotonated forms of all the PLY-based ligands. From this structural analysis of **1–3**, along with their CD spectra analysis, a transformation of a racemate into a pure enantiomer is observed when the 5th C–H of the PLY moiety is substituted by a bulky group –Br. Finally, the catalytic fate of the π-acidic nature of **1–3** was evaluated towards the catalytic α-oxygenation of primary amine using ambient oxygen. The catalyst showed a better and excellent activity for the electronically rich PLY moiety. The catalytic approach was surveyed under wide substrates, such as aryl-, biaryl-, heteroaryl- and aliphatic-methenamine, under the optimised reaction condition, intriguing good to excellent yields with a tolerance of common organic functional groups for the selective α-oxygenation of the primary amine. The mechanistic investigations illuminate the PLY-mediated hydrogen transfer from the methanamine unit involving the dissociation of N–H and C–H bonds in two successive steps, leading to nitrile as the key step, which is subsequently transformed into amide

through hydration. In a nutshell, we designed and developed a catalytic approach by regulating the L–M synergism of the Ru-based catalysts for the selective and sustainable α-oxygenation of primary amine in the presence of ambient O_2 under mild conditions. This synthetic strategy for the selective and efficient transformations of amine to amide may open up new windows for the development of non-innocent ligand-based earth-abundant metal catalysts for value-added organic transformations, which are indeed in progress in our laboratory.

Experimental section

Materials and methods

The dimeric ruthenium precursor [Cl(η^6-Cym)Ru(μ-Cl)$_2$Ru(η^6-Cym)Cl], cinnamoyl chloride, aluminium chloride, 2-methoxynaphthalene, and 2-bromo-6-methoxynaphthalene were purchased from Sigma-Aldrich. Methyl iodide, silver oxide, phenylboronic acid, and $Pd(PPh_3)_4$ were purchased from TCI, India. All other chemicals and solvents were of analytical grade and were used as supplied. The PLY-based ligands HO,O-PLY, HO,O-PLY-Br and HO,O-PLY-Ph were synthesized according to the literature method.[104,105] All the amine substrates were purchased from commercial sources. All the catalytic reactions were accomplished under air. TLC analysis was performed on Merck 60 F254 silica aluminium sheets, and column chromatography was carried out on silica gel (Merck silica gel 60–120 mesh). 1H and $^{13}C\{^1H\}$ NMR spectra were recorded using a Bruker advance 400 MHz spectrometer (Bruker, Massachusetts, USA). Electrospray ionization mass spectra (ESI) were recorded using Shimadzu LCMS 2020 mass spectrometers. The elemental (C, H and N) analyses were performed using a PerkinElmer 2400 CHN micro analyzer (PerkinElmer, Waltham, USA). The infrared spectra were performed using an FTIR-8400S SHIMADZU spectrophotometer (Shimadzu, Kyoto, Japan) with a KBr pellet. EPR spectroscopic measurements were performed using a Magnettech GmbH EPR Spectrometer MiniScope MS400. Electronic absorption spectra were recorded using a HITACHI U-2910 UV-Vis spectrophotometer (Tokyo, Japan). Cyclic voltammetry was performed in DCM with 0.1 M Bu_4NClO_4 as an electrolyte using a three-electrode configuration (Ag/AgCl reference electrode, glassy-carbon working electrode, Pt counter electrode) and a K-Lyte 1.2 potentiostat.

Synthesis of [Ru(η^6-Cym)(O,O-PLY)Cl], 1. A mixture of HO, O-PLY (65 mg, 0.32 mmol) and dimeric ruthenium cymene precursor [$Ru_2(Cym)_2Cl_4$] (100 mg, 0.16 mmol) was dissolved in dry dichloromethane (25 ml) under a nitrogen atmosphere. Then, NEt_3 was added to the reaction mixture, and the solution was left overnight and stirred at room temperature. After completion of the reaction, the resulting deep red solution was concentrated under reduced pressure. When hexane was added to it, a red solid precipitated out from the reaction mixture. The precipitate was filtered, washed with hexane and dried *in vacuo*, leading to pure complex **1**, which was used in catalysis without further purification. Single crystals of **1** were obtained from the slow evaporation of MeOH/DCM (3 : 1) solution at room temperature. Yield: 151 mg, 91%. Elemental analysis calc. (%) for $C_{23}H_{21}ClO_2Ru$: C 59.29, H 4.54; found: C 59.07, H 4.39; ESI-MS: (*m*/*z*): calc. for $C_{23}H_{21}O_2Ru$: 431 [M − Cl]$^+$; found: 430.9. ^{1}H NMR (400 MHz, $CDCl_3$) δ/ppm: 7.83 (s, 1H), 7.81 (d, J = 2.7 Hz, 2H), 7.78 (s, 1H), 7.38 (t, J = 7.5 Hz, 1H), 7.20 (s, 1H), 7.18 (s, 1H), 5.58 (d, J = 6.0, 2H), 5.33 (d, J = 6.0 Hz, 2H), 2.99 (dt, J = 13.9, 6.9 Hz, 1H), 2.19 (s, 3H), 1.37 (d, J = 7.0 Hz, 6H). $^{13}C\{^1H\}$ NMR (101 MHz, $CDCl_3$) δ/ppm: 176.79, 138.39, 131.90, 128.55, 127.62, 125.48, 122.58, 112.71, 100.07, 97.83, 82.77, 79.53, 77.32, 47.87, 30.94, 22.51, 18.23.

Synthesis of [Ru(η^6-Cym)(O,O-PLY-Br)Cl], 2. Complex **2** was synthesized by following the procedure for **1** using HO, O-PLY-Br (90 mg, 0.32 mmol) and a dimeric ruthenium cymene precursor, [$Ru_2(Cym)_2Cl_4$] (100 mg, 0.16 mmol). The compound was isolated as a deep red precipitate. Single crystals were obtained from the slow evaporation of ethyl MeOH/DCM (3 : 1) solution at room temperature. Yield: 168 mg, 89%. Elemental analysis calc. (%) for $C_{23}H_{20}BrClO_2Ru$: C 50.70, H 3.70; found: C 51.03, H 3.85; ESI-MS: (*m*/*z*): calc. for $C_{23}H_{20}BrO_2Ru$: 511 [M − Cl]$^+$; found: 511. ^{1}H NMR (400 MHz, $CDCl_3$) δ/ppm: 7.90 (s, 2H), 7.69 (d, J = 9.4 Hz, 2H), 7.17 (d, J = 9.3 Hz, 2H), 5.59 (d, J = 6.0 Hz, 2H), 5.33 (d, J = 6.0 Hz, 2H), 2.97 (dd, J = 13.9, 6.9 Hz, 1H), 2.35 (s, 3H), 1.37 (d, J = 7.0 Hz, 6H). $^{13}C\{^1H\}$ NMR (101 MHz, $CDCl_3$) δ/ppm: 176.80, 137.16, 133.39, 128.85, 127.29, 126.97, 115.19, 112.22, 110.10, 97.77, 82.33, 79.63, 46.10, 30.94, 22.56, 17.89.

Synthesis of [Ru(η^6-Cym)(O,O-PLY-Ph)Cl], 3. Complex **3** was synthesized by following the procedure for 1 using HO, O-PLY-Ph (88 mg, 0.32 mmol) and dimeric ruthenium cymene precursor [$Ru_2(Cym)_2Cl_4$](100 mg, 0.16 mmol). The compound was isolated as a deep red precipitate. Single crystals were obtained from the slow evaporation of ethyl MeOH/DCM (3 : 1) solution at room temperature. Yield: 162 mg, 86%. Elemental analysis calc. (%) for $C_{29}H_{25}ClO_2Ru$: C 64.26, H 4.65; found: C 64.57, H 4.42; ESI-MS: (*m*/*z*): calc. for $C_{29}H_{25}O_2Ru$: 507 [M − Cl]$^+$; found: 507. ^{1}H NMR (400 MHz, $CDCl_3$) δ/ppm: 8.05 (s, 2H), 7.86 (d, J = 9.3 Hz, 2H), 7.70 (d, J = 7.5 Hz, 2H), 7.50 (t, J = 7.6 Hz, 2H), 7.39 (t, J = 7.4 Hz, 1H), 7.22 (d, J = 9.3 Hz, 2H), 5.60 (d, J = 5.9 Hz, 2H), 5.34 (d, J = 5.9 Hz, 2H), 3.04–2.96 (m, 1H), 2.37 (s, 3H), 1.38 (d, J = 6.9 Hz). $^{13}C\{^1H\}$ NMR (101 MHz, $CDCl_3$) δ/ppm: 176.72, 140.09, 138.41, 135.58, 130.23, 128.97, 128.67, 127.91, 127.62, 127.37, 127.08, 125.8, 112.42, 97.64, 82.67, 79.49, 45.95, 30.85, 22.40, 18.09.

X-ray crystal structure details of complex 1–3

X-ray diffraction data for the suitable single-crystals of **1–3** were collected using a Bruker-Kappa APEX II CCD diffractometer equipped with a 1 K charge-coupled device (CCD) area detector by employing graphite monochromated Mo-Kα radiation ($k\frac{1}{4}$ 0.71073 Å) at 100.0(2) K. The cell parameters and the reduction and correction of the collected data were determined by SMART SAINTPLus software,[106,107] followed by absorption corrections using SADABS[108] software. Finally, the structure was solved by applying the direct method with the SHELXL-97 program package.[109] The refinement using the full-matrix

least-squares method was executed on all $F2$ data with SHELXL-97. For all non-hydrogen atoms, anisotropic refinement was performed. Subsequently, the additional hydrogen atoms were positioned using the riding model. The molecular graphics were created using mercury software.

General procedure for aerobic oxidation of primary amines to amides

In a 15 mL oven-dried pressure tube containing a magnetic stirring bar, 3 mol% of catalyst (complex **1** or **2** or **3**) and 40 mol% of base (KO^tBu) were dissolved in toluene (3 mL). After stirring for a few minutes, 0.5 mmol of primary amine was added to the reaction mixture and stirred for 15 h at 90 °C under aerobic conditions. After completion of the conversion, the amide product was extracted with 15 mL (3 × 5 mL) of ethyl acetate, and the combined organic layers were dried over anhydrous Na_2SO_4. The solvent was evaporated under reduced pressure, leading to the crude amide, which was further purified by column chromatography on silica using hexane/ethyl acetate as an eluent.

Author contributions

Nilaj Bandopadhyay: Conceptualization, formal analysis, methodology, investigation; Krishnendu Paramanik: formal analysis, investigation; Gayetri Sarkar: formal analysis, visualization; Suvojit Roy: formal analysis, validation; Subhra Jyoti Panda: formal analysis, validation; Chandra Shekhar Purohit: formal analysis, validation; Bhaskar Biswas: conceptualization, writing-reviewing and editing, supervision; Hari Sankar Das: conceptualization, writing-reviewing and editing, supervision.

Data availability

Data will be made available on request.

Conflicts of interest

There are no conflicts of interest.

Acknowledgements

HSD and NB acknowledge Science and Engineering Research Board (SERB), India for financial support under EMEQ scheme (EEQ/2019/000374 and EEQ/2023/0000440). KP thanks CSIR-India and GS thanks UGC-India for fellowship.

References

1 A. Greenberg, C. M. Breneman and J. F. Liebman, *Biochemistry and Materials Science*, Wiley, New York, 2000.
2 B. L. Deopura, B. Gupta, M. Joshi and R. Alagirusami, *Polyesters and Polyamides*, CRC Press, Boca Raton, 2008.
3 D. Lipp, in *Encyclopedia of Chemical Technology*, ed. J. I. Kroschwitz, John Wiley & Sons, New York, 1991, vol. 1, p. 266.
4 J. M. Humphrey and A. R. Chamberlin, *Chem. Rev.*, 1997, **97**, 2243.
5 N. Schneider, D. M. Lowe, R. A. Sayle, M. A. Tarselli and G. A. Landrum, *J. Med. Chem.*, 2016, **59**, 4385.
6 T. J. Deming, *Prog. Polym. Sci.*, 2007, **32**, 858.
7 R. C. Larock, *Comprehensive Organic Transformations*, Wiley-VCH, New York, 2nd edn, 1999.
8 N. Sewald and H. D. Jakubke, *Peptides: Chemistry and Biology*, Wiley-VCH, Weinheim, 2002.
9 T. Cupido, J. T. Puche, J. Spengler and F. Albericio, *Curr. Opin. Drug Discovery Dev.*, 2007, **10**, 768.
10 A. Kumar, N. A. E. Jalapa, G. Leitus, Y. D. Posner, L. Avram and D. Milstein, *Angew. Chem., Int. Ed.*, 2017, **56**, 14992.
11 H. Charville, D. A. Jackson, G. Hodges, A. Whiting and M. R. Wilson, *Eur. J. Org. Chem.*, 2011, 5981.
12 L. J. Goossen, D. M. Ohlmann and P. P. Lange, *Synthesis*, 2009, 160.
13 R. S. Varma, *Green Chem.*, 1999, **1**, 43.
14 L. Perreux, A. Loupy and F. Volatron, *Tetrahedron*, 2002, **58**, 2155.
15 M. B. Smith and J. March, *March's Advanced Organic Chemistry*, Wiley, New York, 5th edn, 2001.
16 M. B. Smith, *Organic Synthesis*, Mc-Graw-Hill, New York, 2nd edn, 2002.
17 L. U. Nordstrøm, H. Vogt and R. Madsen, *J. Am. Chem. Soc.*, 2008, **52**, 17672.
18 S. C. Ghosh, S. Muthaiah, Y. Zhang, X. Xu and S. H. Hong, *Adv. Synth. Catal.*, 2009, **351**, 2643.
19 Y. Wang, D. Zhu, L. Tang, S. Wang and Z. Wang, *Angew. Chem., Int. Ed.*, 2011, **50**, 8917.
20 D. Srimani, E. Balaraman, P. Hu, Y. B. David and D. Milstein, *Adv. Synth. Catal.*, 2013, **355**, 2525.
21 S. L. Zultanski, J. Zhao and S. S. Stahl, *J. Am. Chem. Soc.*, 2016, **138**, 6416.
22 J. Luo, Q.-Q. Zhou, M. Montag, Y. Ben-Davida and D. Milstein, *Chem. Sci.*, 2022, **13**, 3894.
23 P. Daw, A. Kumar, N. A. E. Jalapa, Y. B. David and D. Milstein, *J. Am. Chem. Soc.*, 2019, **141**, 12202.
24 S. Kar, Y. Xie, Q. Q. Zhou, Y. D. Posner, Y. B. David and D. Milstein, *ACS Catal.*, 2021, **11**, 7383.
25 X. F. Wu, M. Sharif, J. B. Feng, H. Neumann, A. P. Davtyan, P. Langer and M. Beller, *Green Chem.*, 2013, **15**, 1956.
26 Z. Xie, R. Chen, Z. Du, L. Kong, Z. Li, Z. Li, N. Wang and J. Liu, *Asian J. Org. Chem.*, 2017, **6**, 157.
27 K. Yamaguchi, H. Kobayashi, T. Oishi and N. Mizuno, *Angew. Chem., Int. Ed.*, 2012, **51**, 544.
28 J. R. Martinelli, T. P. Clark, D. A. Watson, R. H. Munday and S. L. Buchwald, *Angew. Chem., Int. Ed.*, 2007, **46**, 8460.
29 A. Brennführer, H. Neumann and M. Beller, *Angew. Chem., Int. Ed.*, 2009, **48**, 4114.

30 C. W. Cheung, M. L. Ploeger and X. Hu, *Chem. Sci.*, 2018, **9**, 655.
31 A. M. Veatch and E. J. Alexanian, *Chem. Sci.*, 2020, **11**, 7210.
32 P. Wang, Z. Cao, Y. X. Wang, H. Neumann and M. Beller, *Eur. J. Org. Chem.*, 2022, e202200663.
33 S. H. Cho, E. J. Yoo, I. Bae and S. Chang, *J. Am. Chem. Soc.*, 2005, **127**, 16046.
34 S. Chang, M. Lee, D. Y. Jung, E. J. Yoo, S. H. Cho and S. K. Han, *J. Am. Chem. Soc.*, 2006, **128**(38), 12366.
35 Z. W. Chen, H. F. Jiang, X. Y. Pan and Z. J. He, *Tetrahedron*, 2011, **67**, 5920.
36 S. L. Shi and S. Buchwald, *Nat. Chem.*, 2015, **7**, 38.
37 S. E. Eldred, D. A. Stone, S. H. Gellman and S. S. Stahl, *J. Am. Chem. Soc.*, 2003, **125**, 3422.
38 T. A. Dineen, M. A. Zajac and A. G. Myers, *J. Am. Chem. Soc.*, 2006, **128**, 16406.
39 M. Zhang, S. Imm, S. Bähn, L. Neubert, H. Neumann and M. Beller, *Angew. Chem., Int. Ed.*, 2012, **51**, 3905.
40 M. Tamura, T. Tonomura, K. I. Shimizu and A. Satsuma, *Green Chem.*, 2012, **14**, 717.
41 C. L. Allen, B. N. Atkinson and J. M. J. Williams, *Angew. Chem., Int. Ed.*, 2012, **51**, 1383.
42 L. B. Figueroa, A. O. Porras and D. G. Sánchez, *J. Org. Chem.*, 2014, **79**, 4544.
43 G. Li and M. Szostak, *Synthesis*, 2020, 2579.
44 W. J. Yoo and C. J. Li, *J. Am. Chem. Soc.*, 2006, **128**, 13064.
45 W. K. Chan, C. M. Ho, M. K. Wong and C. M. Che, *J. Am. Chem. Soc.*, 2006, **128**, 14796.
46 H. U. Vora and T. Rovis, *J. Am. Chem. Soc.*, 2007, **129**, 13796.
47 J. W. Bode and S. S. Sohn, *J. Am. Chem. Soc.*, 2007, **129**, 13798.
48 Y. Suto, N. Yamagiwa and Y. Torisawa, *Tetrahedron Lett.*, 2008, **49**, 5732.
49 K. E. Kovi and C. Wolf, *Chem. – Eur. J.*, 2008, **14**, 6302.
50 J. Li, F. Xu, Y. Zhang and Q. Shen, *J. Org. Chem.*, 2009, **74**, 2575.
51 S. De Sarkar and A. Studer, *Org. Lett.*, 2010, **12**, 1992.
52 S. C. Ghosh, J. S. Y. Ngiam, A. M. Seayad, D. T. Tuan, C. L. L. Chai and A. Chen, *J. Org. Chem.*, 2012, **77**, 8007.
53 O. P. S. Patel, D. Anand, R. K. Maurya and P. P. Yadav, *Green Chem.*, 2015, **17**, 3728.
54 H. Fujiwara, Y. Ogasawara, K. Yamaguchi and N. Mizuno, *Angew. Chem., Int. Ed.*, 2007, **46**, 5202.
55 N. A. Owston, A. J. Parker and J. M. J. Williams, *Org. Lett.*, 2007, **9**, 3599.
56 M. A. Ali and T. Punniyamurthy, *Adv. Synth. Catal.*, 2010, **352**, 288.
57 P. Crochet and V. Cadierno, *Chem. Commun.*, 2015, **51**, 2495.
58 P. J. G. Liste, V. Cadierno and S. E. G. Garrido, *ACS Sustainable Chem. Eng.*, 2015, **3**, 3004.
59 G. C. Midya, A. Kapat, S. Maiti and J. Dash, *J. Org. Chem.*, 2015, **80**, 4148.
60 A. B. Szafran, K. Erfurt, M. S. Kwasny, T. Piotrowski and A. Chrobok, *ACS Sustainable Chem. Eng.*, 2022, **10**, 13568.
61 D. D. S. Sharley and J. M. J. Williams, *Tetrahedron Lett.*, 2017, **58**, 4090.
62 X. Xing, C. Xu, B. Chen, C. Li, S. C. Virgil and R. H. Grubbs, *J. Am. Chem. Soc.*, 2018, **140**, 17782.
63 B. Paul, M. Maji and S. Kundu, *ACS Catal.*, 2019, **9**, 10469.
64 B. Guo, J. G. de Vries and E. Otten, *Chem. Sci.*, 2019, **10**, 10647.
65 H. Naka and A. Naraoka, *Tetrahedron Lett.*, 2020, **61**, 151557.
66 S. Yadav and R. Gupta, *Inorg. Chem.*, 2022, **61**, 15463.
67 Y. Wang, D. Zhu, L. Tang, S. Wang and Z. Wang, *Angew. Chem., Int. Ed.*, 2011, **50**, 8917, (*Angew. Chem.*, 2011, **123**, 9079).
68 K. Yamaguchi, M. Matsushita and N. Mizuno, *Angew. Chem., Int. Ed.*, 2004, **43**, 1576, (*Angew. Chem.*, 2004, **116**, 1602).
69 S. L. Buchwald, C. Mauger, G. Mignani and U. Scholz, *Adv. Synth. Catal.*, 2006, **348**, 23.
70 T. E. Müller and M. Beller, *Chem. Rev.*, 1998, **98**, 675.
71 C. Gunanathan and D. Milstein, *Angew. Chem., Int. Ed.*, 2008, **47**, 8661.
72 F. Chen, C. Topf, J. Radnik, C. Kreyenschulte, H. Lund, M. Schneider, A. E. Surkus, L. He, K. Junge and M. Beller, *J. Am. Chem. Soc.*, 2016, **138**, 8781.
73 S. Zhou, K. Junge, D. Addis, S. Das and M. Beller, *Angew. Chem., Int. Ed.*, 2009, **48**, 9507.
74 C. Cheng and M. Brookhart, *J. Am. Chem. Soc.*, 2012, **134**, 11304.
75 S. Das, H. S. Das, B. Singh, R. K. Haridasan, A. Das and S. K. Mandal, *Inorg. Chem.*, 2019, **58**, 11274.
76 H. S. Das, S. Das, K. Dey, B. Singh, R. K. Haridasan, A. Das, J. Ahmed and S. K. Mandal, *Chem. Commun.*, 2019, **55**, 11868.
77 X. Huang and J. T. Groves, *Chem. Rev.*, 2018, **118**, 2491.
78 J. W. Kim, K. Yamaguchi and N. Mizuno, *Angew. Chem., Int. Ed.*, 2008, **47**, 9249.
79 X. Jin, K. Kataoka, T. Yatabe, K. Yamaguchi and N. Mizuno, *Angew. Chem., Int. Ed.*, 2016, **55**, 7212.
80 T. Hirao, T. Amaya and T. Ito, *Heterocycles*, 2012, **86**, 927.
81 M. H. So, Y. Liu, C. M. Ho and C. M. Che, *Chem. – Asian J.*, 2009, **4**, 1551.
82 H. Miyamura, M. Morita, T. Inasaki and S. Kobayashi, *Bull. Chem. Soc. Jpn.*, 2011, **84**, 588.
83 P. Preedasuriyachai, W. Chavasiri and H. Sakurai, *Synlett*, 2011, 1121.
84 Y. Wang, H. Kobayashi, K. Yamaguchi and N. Mizuno, *Chem. Commun.*, 2012, **48**, 2642.
85 H. Wang, L. Wang, S. Wang, X. Dong, J. Zhang and F. S. Xiao, *ChemCatChem*, 2019, **11**, 401.
86 E. R. Klobukowski, M. L. Mueller, R. J. Angelici and L. K. Woo, *ACS Catal.*, 2011, **1**, 703.
87 W. Xu, Y. Y. Jiang and H. Fu, *Synlett*, 2012, 801.
88 R. Ray, A. S. Hazari, S. Chandra, D. Maiti and G. K. Lahiri, *Chem. – Eur. J.*, 2018, **24**, 1067.
89 X. Yan, Q. Dong, Y. Li, L. Meng, Z. Hao, Z. Han, G. L. Lu and J. Lin, *Dalton Trans.*, 2020, **49**, 3480.

90 S. Yadav, N. U. D. Reshi, S. Pal and J. K. Bera, *Catal. Sci. Technol.*, 2021, **11**, 7018.
91 A. Mukherjee, S. C. Sau and S. K. Mandal, *Acc. Chem. Res.*, 2017, **50**, 1679.
92 A. Banik, J. Ahmed, S. Sil and S. K. Mandal, *Chem. Sci.*, 2021, **12**, 8353.
93 K. Paramanik, N. Bandopadhyay, G. Sarkar, S. Chatterjee, S. Roy, S. J. Panda, C. S. Purohit, B. Biswas and H. S. Das, *Dalton Trans.*, 2023, **52**, 4964.
94 N. Bandopadhyay, K. Paramanik, G. Sarkar, S. Chatterjee, S. Roy, S. J. Panda, C. S. Purohit, B. Biswas and H. S. Das, *New J. Chem.*, 2023, **47**, 9414.
95 G. Sarkar, N. Bandopadhyay, K. Paramanik, S. Saha, S. J. Panda, C. S. Purohit, B. Biswas and H. S. Das, *Mol. Catal.*, 2023, **545**, 113212.
96 D. Schweinfurth, H. S. Das, F. Weisser, D. Bubrin and B. Sarkar, *Inorg. Chem.*, 2011, **50**(3), 1150.
97 B. L. Rivera, V. Jancik, R. M. Esparza, D. M. Otero and J. H. Trujillo, *Chem. – Eur. J.*, 2021, **27**, 1912.
98 J. T. Muckerman, D. E. Polyansky, T. Wada, K. Tanaka and E. Fujita, *Inorg. Chem.*, 2008, **47**, 1787.
99 B. L. Tran, M. Pink and D. J. Mindiola, *Organometallics*, 2009, **28**, 2234.
100 A. De, M. Garai, H. R. Yadav, A. R. Choudhury and B. Biswas, *Appl. Organomet. Chem.*, 2017, **31**, e3551.
101 B. Chowdhury, B. Bhowmik, A. Sahu, M. Joshi, S. Paul, A. R. Choudhury and B. Biswas, *J. Chem. Sci.*, 2018, **130**, 161.
102 M. Garai, A. Das, M. Joshi, S. Paul, M. Shit, A. R. Choudhury and B. Biswas, *Polyhedron*, 2018, **156**, 223.
103 M. Wang, S. Qiu, H. Yang, Y. Huang, L. Dai, B. Zhang and J. Zou, *Chemosphere*, 2021, **270**, 129448.
104 M. Bhunia, S. R. Sahoo, B. K. Shaw, S. Vaidya, A. Pariyar, G. Vijaykumar, D. Adhikari and S. K. Mandal, *Chem. Sci.*, 2019, **10**, 7433.
105 L. Bensch, I. Gruber, C. Janiak and T. J. J. Mueller, *Chem. – Eur. J.*, 2017, **23**, 10551.
106 *SMART, Version 5.0*, Bruker AXS, Inc., Analytical X-ray Systems, 5465 East Cheryl Parkway, Madison, WI 53711-5373, 2000.
107 *SAINT, Version 6.02*, Bruker AXS, Inc., Analytical X-ray Systems, 5465 East Cheryl Parkway, Madison, WI 53711-5373, 2000.
108 G. M. Sheldrick, *Program for Empirical Absorption Correction of Area Detector Data*, Universität Göttingen, Germany, 1996.
109 G. M. Sheldrick, *SHELXL 97, Program for crystal structure refinement*, University of Göttingen, Göttingen, Germany, 1997.